# The effects of plasma from patients with active thyroid-associated orbitopathy on the survival and inflammation of melanoma-associated fibroblasts

Huifang Chen[1,2,*], Shiyuan Chen[2,*] and Zhenfeng Liu[2]

[1] Department of Medicine, Guangxi University of Science and Technology, Liuzhou, China
[2] Department of Traditional Chinese Medicine, The Second Affiliated Hospital of Guangxi University of Science and Technology, Liuzhou, China
[*] These authors contributed equally to this work.

## ABSTRACT

**Background:** Plasma from patients with active thyroid-associated orbitopathy (TAO-A) could cause inflammation to fibroblasts, and such a mechanism was explored in the context of melanoma.

**Methods:** Plasma samples collected from TAO-A patients and healthy control (HC) were primarily co-cultured with the melanoma-associated fibroblasts (MAFs) derived from melanoma patients. The survival and inflammation of the co-cultured MAFs were measured after confirming the levels of pro-inflammatory cytokines. Ki67 and Vimentin (VIM) markers were analyzed by immunofluorescence, and cell survival and migration were assessed using cell counting kit-8 (CCK-8) and Transwell. The THP-1 cells were induced to differentiate into macrophages, which were subsequently co-cultured to assess M1/M2 polarization status. Meanwhile, the levels of inflammatory factor were detected by enzyme-linked immunosorbent assay (ELISA). The gene expression was measured by reverse transcription quantitative PCR (RT-qPCR), and the activation of PI3K/AKT, STAT1, p65, and ERK signaling pathways was detected by Western Blot.

**Results:** Plasmas derived from TAO-A patients were characterized by elevated levels of pro-inflammatory cytokines, which enhanced the inflammation status and survival of MAFs, promoted the levels of PI3K and AKT, and downregulated expression of Bax. The co-culture of the plasma with MAFs evidently promoted M1 polarization and the phosphorylation of STAT1, P65 and ERK1/2.

**Conclusion:** These findings proved the effects of the plasmas of TAO-A patients on the survival and inflammation of MAFs, providing evidence for future studies to delve into the relevant mechanisms.

**Subjects** Cell Biology, Immunology, Oncology

**Keywords** Melanoma, Tumor microenvironment, Melanoma-associated fibroblasts, Inflammation, Survival

## INTRODUCTION

Recent studies have shown that the tumor microenvironment (TME) plays an indispensable role as a potential therapeutic target in cancers (*Pitt et al., 2016*), and that

Submitted 26 August 2024
Accepted 8 November 2024
Published 27 November 2024

Corresponding author
Zhenfeng Liu,
lzf18077229888@126.com

Academic editor
Fanglin Guan

Additional Information and Declarations can be found on page 14

DOI **10.7717/peerj.18612**

stromal cells of the TME are decisive to tumor progression and unsatisfactory treatment outcome (*Junttila & de Sauvage, 2013*). The TME contains both non-cancerous cells and components that could drive the growth, invasion, metastasis, and response of tumor cells to therapies (*Xiao & Yu, 2021*; *Elhanani, Ben-Uri & Keren, 2023*). A variety of cell types, including tumor-infiltrating immune cells, cancer-associated fibroblasts (CAFs) and endothelial cells of extracellular matrix, are present in the TME (*Arneth, 2019*; *Meng et al., 2024*; *Zhang et al., 2024*). Hence, a close interaction between the TME and tumor cells could promote tumorigenesis (*Hajdara et al., 2023*).

Thyroid-associated orbitopathy (TAO-A), also known as Graves' ophthalmopathy, is an autoimmune disease correlated with thyroid dysfunction (*Bahn, 2010*). A distinguishing feature of TAO-A is the swelling of orbital tissue, which includes both extraocular adipose and muscle tissues. Soft tissue swelling is a result of the accumulation of nonsulfated glycosaminoglycans, inflammation, hyaluronan, and activation of local fibroblasts (*Berchner-Pfannschmidt et al., 2016*; *Wang et al., 2023*). If left untreated, the swelling of orbital tissue can lead to orbital congestion, exophthalmos, compressive neuropathy, and ultimately vision loss (*Wang et al., 2021*). Melanoma is a skin cancer resulted from malignant transformation of melanocytes, which are a type of cells with pigment-producing ability (*Ahmed, Qadir & Ghafoor, 2020*; *Schadendorf et al., 2018*). Patients at an early stage can be successfully treated with surgery but the survival outcomes could be sharply reduced by the occurrence of metastasis (*Davis, Shalin & Tackett, 2019*). Melanoma is one of the most immunogenic tumor types and is more likely to respond actively to immunotherapy due to its well-expressed lymphoid infiltration (*Tagliaferri et al., 2022*; *Marzagalli, Ebelt & Manuel, 2019*). However, similar to other cancer types, melanoma cells acquire a variety of suppressive properties to escape from both innate and adaptive immune recognition and destruction (*Marzagalli, Ebelt & Manuel, 2019*).

Melanoma-associated fibroblasts (MAFs) refer to a melanoma-driven distinct subpopulation of CAFs that promote tumorigenesis through facilitating immune evasion and proliferation of tumor cells (*Papaccio et al., 2021*; *Eble & Niland, 2019*). Though MAFs share some basic characteristics with CAFs, MAFs also undergo some molecular changes to adapt their functions to particular requirements of melanoma cells (*Romano et al., 2021*), significantly contributing to the structural alternations of microenvironment and some molecular and cellular alternations related to the outcome of melanoma (*Bellei, Migliano & Picardo, 2020*). MAFs enhance the proliferation and invasiveness of melanoma cells and promote their resistance to anti-apoptosis by secreting growth factors (*e.g.*, TGF-β) and extracellular matrix proteins (*Brenner et al., 2005*). In addition, MAFs can secrete pro-angiogenic factors to increase the formation of neovascularization in the tumor, providing nutrients and oxygen to the tumor to support its growth and spread (*Sala et al., 2002*). At present, most studies have analyzed the tumor-promoting role of MAFs in melanoma (*Lian et al., 2024*; *Shi et al., 2023*). This study set out to explore the effects of plasma from TAO-A patients on the survival, migration and inflammatory response of MAFs, and to further analyze whether such an effect was mediated through modulating PI3K/AKT signaling pathway and promoting M1 polarization in macrophages. The

current findings contributed to the understanding on the association between TAO-A and tumors and provided novel targets for future research and therapy for melanoma.

## MATERIALS AND METHODS

### Ethic statement

The current study obtained the approval from the Ethic Committee of our hospital and all the participants enrolled in this study signed the written informed consent. All the experiments were carried out strictly following relevant regulations and guidelines. The study was approved by Guangxi University of Science and Technology Medical Ethics Committee (No. YX20230301H015).

### Human sample collection

Human blood samples were collected from patients with TAO-A and HC ($n$ = 5 for each group) as needed. In detail, 4 mL venous blood was collected into the blood collection tubes containing ethylenediaminetetraacetic acid (EDTA, E8040; Solarbio Lifesciences, Beijing, China). Then the plasma was obtained *via* centrifugation at 3,000 rpm for 10 minutes (min) at 4 °C and stored at −80 °C for subsequent analysis.

MAFs used in this assay were isolated from primary tumors of melanoma patients ($n$ = 3) (*Çakır et al., 2021*). In detail, the inner tumor mass was minced into approximately 1 $mm^3$ and digested in 20 mL Dulbecco's modified Eagle's medium (DMEM, 21063-029; Thermo Fisher Scientific, Waltham, MA, USA) supplemented with 0.6 U/mL dispase (17105-041; Thermo Fisher Scientific, Waltham, MA, USA) and 200 U/mL collagenase IV (17104-019; Thermo Fisher Scientific, Waltham, MA, USA). Differential adhesion/trypsinization method was employed to separate MAFs from the melanoma cells. Briefly, the tumor cell suspension digested in collagenase IV and dispase was plated into the plastic cell culture dishes for 30 min. Hereafter, adherent cells were cultured for differential adhesion after the removal of floating cells. After that, subconfluent cell culture was trypinsized for 1 min to eliminate detached cells, while the adherent cells enriched in MAFs were subcultured for differential adhesion again. For the assays in this study, MAFs grown until the confluence of 75–80% were rinsed in phosphate-buffered saline (PBS) and further cultured in 10 mL basal medium consisting of standard DMEM, 20% fetal bovine serum (FBS, 10437-036; Thermo Fisher Scientific, Waltham, MA, USA), 1% penicillin-streptomycin (15070-063; Thermo Fisher Scientific, Waltham, MA, USA) and 1% L-glutamine (21051-024; Thermo Fisher Scientific, Waltham, MA, USA).

### Cell culture and induction

Here, we used THP-1 monocytes as a macrophage model to investigate the effect of plasma on macrophage polarization in TAO-A patients. The complete medium containing 90% Roswell Park Memorial Institute-1640 medium (11875-093; Thermo Fisher Scientific, Waltham, MA, USA), 10% FBS and 0.05 mM 2-mercaptoethanol (21985-023; Thermo Fisher Scientific, Waltham, MA, USA) was used to culture human monocytes THP-1 (SCSP-567; National Collection of Authenticated Cell Cultures, Shanghai, China) at 37 °C with 5% $CO_2$. All the cells were identified by STR profiling and tested negative for

mycoplasma contamination. For the induction into macrophages, THP-1 monocytes were treated with phorbol-12-myristate-13-acetate (PMA) at 100 ng/mL (HY-18739; MedChemExpress, Monmouth Junction, NJ) for 24 hours (h) (*Park et al., 2023*). Routine testing for mycoplasma was conducted on all the cell lines.

## Cell viability assay

The CCK-8 test was used to assess the effect of plasma from TAO-A patients on the survival of MAFs. A total of $2 \times 10^3$ MAFs following the co-culture with the plasma were seeded for culture in independent triplicates for the culture of 0, 12, 24, 36 and 48 h, followed by the addition of 10-μ LCCK-8 working solution (CK04; Donjido, Kumamoto, Japan) and incubation for 3 h at 37 °C. The absorbance in each well was read at 450 nm using a microplate reader (iMark, Bio-Lad Laboratories, Inc., Hercules, CA, US).

## Cell migration assay

Transwell assay was used to assess the migratory ability of plasma to MAFs in TAO-A patients. Cell migration assay was carried out utilizing a transwell chamber (8-μm pore size; EMD Millipore, Darmstadt, Germany). For migration assay, $3 \times 10^4$ MAFs in serum-free culture medium (200 μL) were seeded into the upper chamber, while the complete medium containing 10% FBS (700 μL) was added into the lower chamber. Subsequently, the chamber was incubated at 37 °C for 48 h, and the migrated cells were fixed by 4% paraformaldehyde (P1110; Solarbio Lifesciences, Beijing, China) at ambient temperature for 15 min. 0.1% crystal violet staining solution (G1063; Solarbio Lifesciences, Beijing, China) was applied for the staining of these cells at room temperature for 30 min, and the cells were visualized and counted under an inverted light microscope (Eclipse TS100; Nikon Corporation, Tokyo, Japan).

## Cell immunofluorescence assay

MAFs or induced macrophages were seeded into the 24-well plates and cultured at 37 °C for 24 h. Hereafter, the cells were fixed in 4% paraformaldehyde for 10 min, blocked in 1% bovine serum albumin (IA0910; Solarbio Lifesciences, Beijing, China) for 30 min, and incubated with fluorescence-labeled primary antibodies at 4 °C overnight and then with secondary antibody at ambient temperature for 30 min in the dark. Next, glycerol (S2150; Solarbio Lifesciences, Beijing, China) was used to mount the cells, which were observed under a Zeiss LSM 510 fluorescence microscope (Carl Zeiss, Jena, Germany). The information of antibodies applied was listed in Table 1.

## ELISA

The contents of inflammatory cytokines including interleukin (IL)-1β (PI305), IL-6 (PI330), TNF-α (PT518), TGF-β (PT880) and IL-18 (PI558) within the plasma sample were quantified using the relevant ELISA assay kit purchased from Beyotime Institute (Shanghai, China) following the manuals.

**Table 1** Information of antibodies.

| Antibody | Host species | Label | Dilution ratio | Catalog number and manufacturer | Application |
|---|---|---|---|---|---|
| Anti-Ki67 antibody | Rabbit | Alexa Fluor® 488 | 1:100 | ab197234, Abcam | Cell immunofluorescence assay |
| Anti-Vimentin antibody | Rabbit | Alexa Fluor® 647 | 1:100 | ab194719, Abcam | Cell immunofluorescence assay |
| Anti-CD86 antibody | Rabbit | Alexa Fluor® 488 | 1:50 | ab290990, Abcam | Cell immunofluorescence assay |
| Anti-CD206 antibody | Rabbit | Alexa Fluor® 488 | 1:200 | #36508, Cell Signaling Technology | Cell immunofluorescence assay |
| Anti-CD11B antibody | Rabbit | Alexa Fluor® 647 | 1:200 | NB110-89474AF647, Novus Biologicals | Cell immunofluorescence assay |
| Goat anti-rabbit IgG H&L | Goat | / | 1:2,000 | ab6702, Abcam | Cell immunofluorescence assay |
| Anti-PI3K antibody | Rabbit | / | 1:1,000 | #4292, Cell Signaling Technology | Western blotting |
| Anti-p-PI3K antibody | Rabbit | / | 1:1,000 | ab182651, Abcam | Western blotting |
| Anti-p-AKT antibody | Rabbit | / | 1:2,000 | #4060, Cell Signaling Technology | Western blotting |
| Anti-AKT antibody | Rabbit | / | 1:1,000 | #4685, Cell Signaling Technology | Western blotting |
| Anti-BAX antibody | Rabbit | / | 1:10,000 | ab32503, Abcam | Western blotting |
| Anti-p-STAT1 antibody | Rabbit | / | 1:10,000 | ab109461, Abcam | Western blotting |
| Anti-STAT1 antibody | Rabbit | / | 1:10,000 | ab109320, Abcam | Western blotting |
| Anti-P65 antibody | Rabbit | / | 1:10,000 | ab32536, Abcam | Western blotting |
| Anti-p-P65 antibody | Rabbit | / | 1:1,000 | ab76302, Abcam | Western blotting |
| Anti-ERK1/2 antibody | Rabbit | / | 1:10,000 | ab184699, Abcam | Western blotting |
| Anti-p-ERK1/2 | Rabbit | / | 1:2,000 | #4370, Cell Signaling Technology | Western blotting |
| Anti-GAPDH antibody | Rabbit | / | 1:5,000 | ab181602, Abcam | Western blotting |
| Goat anti-rabbit IgG H&L | Goat | HRP | 1:2,000 | ab205718, Abcam | Western blotting |

## Western blotting

Cells were lysed in RIPA lysis buffer (R0010; Solarbio Lifesciences, Beijing, China) and the protein concentrations were tested using BCA protein assay kit (PC0020; Solarbio Lifesciences, Beijing, China). Next, cell lysates were resolved *via* SDS-PAGE separation gel and transferred onto polyvinylidene difluoride (PVDF) membranes (YA1701; Solarbio Lifesciences, Beijing, China), which were blocked with 5% non-fat milk and probed with the primary antibodies at required dilution ratio at the temperature of 4 °C overnight. Horseradish peroxidase-conjugated secondary antibody was applied for amplifying the signals. Immunodetection was achieved using an ECL visualization agent (PE0010; Solarbio Lifesciences, Beijing, China) and ChemiDoc Imaging Systems (Bio-Rad Laboratories, Inc., Hercules, CA, USA). Finally, the densitometry on the protein bands was analyzed using ImageJ software 5.0 (Bio-Rad Laboratories, Inc., Hercules, CA, USA). See Table 1 for the information of antibodies.

**Table 2** Sequences of primers in qPCR assay.

| Gene name/NCBI ID | Primers |
|---|---|
| IL1B (3553) | |
| Forward | 5′-CCACAGACCTTCCAGGAGAATG-3′ |
| Reverse | 5′-GTGCAGTTCAGTGATCGTACAGG-3′ |
| IL6 (3569) | |
| Forward | 5′-AGACAGCCACTCACCTCTTCAG-3′ |
| Reverse | 5′-TTCTGCCAGTGCCTCTTTGCTG-3′ |
| IL18 (3606) | |
| Forward | 5′-GATAGCCAGCCTAGAGGTATGG-3′ |
| Reverse | 5′-CCTTGATGTTATCAGGAGGATTCA-3′ |
| TGFB (7040) | |
| Forward | 5′-TACCTGAACCCGTGTTGCTCTC-3′ |
| Reverse | 5′-GTTGCTGAGGTATCGCCAGGAA-3′ |
| MYBPC3 (4607) | |
| Forward | 5′-AACCTGTCAGCCAAGCTCCACT-3′ |
| Reverse | 5′-CCACAATGGTGTCTGGTATGCG-3′ |
| COL1A1 (1277) | |
| Forward | 5′-GATTCCCTGGACCTAAAGGTGC-3′ |
| Reverse | 5′-AGCCTCTCCATCTTTGCCAGCA-3′ |
| ACTA2 (59) | |
| Forward | 5′-CTATGCCTCTGGACGCACAACT-3′ |
| Reverse | 5′-CAGATCCAGACGCATGATGGCA-3′ |
| VEGFA (7422) | |
| Forward | 5′-TTGCCTTGCTGCTCTACCTCCA-3′ |
| Reverse | 5′-GATGGCAGTAGCTGCGCTGATA-3′ |
| GAPDH (2597) | |
| Forward | 5′-GTCTCCTCTGACTTCAACAGCG -3′ |
| Reverse | 5′-ACCACCCTGTTGCTGTAGCCAA-3′ |

## RNA separation, cDNA synthesis and RT-qPCR

Rneasy Mini Kit (74104; Qiagen, Hilden, Germany) was employed to isolate total RNA from cells and total RNA (1 μg) was applied for the synthesis of cDNA utilizing the iScript™ cDNA Synthesis Kit (1708890; Bio-Rad Laboratories, Inc., Hercules, CA, USA) RT-qPCR was then carried out using iQ SYBR Green Master Mix (1708887; Bio-Rad Laboratories, Inc., Hercules, CA, USA) in CFX384 Touch Real-Time PCR System (Bio-Rad Laboratories, Inc., Hercules, CA, USA) at the following parameters for thermal cycling: at 95 °C for 3 min, and 40 repeated cycles at 95 °C for 10 seconds (s) and at 60 °C for 30 s. $2^{-\Delta\Delta Ct}$ method was applied for calculating the relative mRNA levels, with GAPDH as a normalization control (*Livak & Schmittgen, 2001*; *Amuthalakshmi, Sindhuja & Nalini, 2022*). All primer sequences are shown in Table 2.

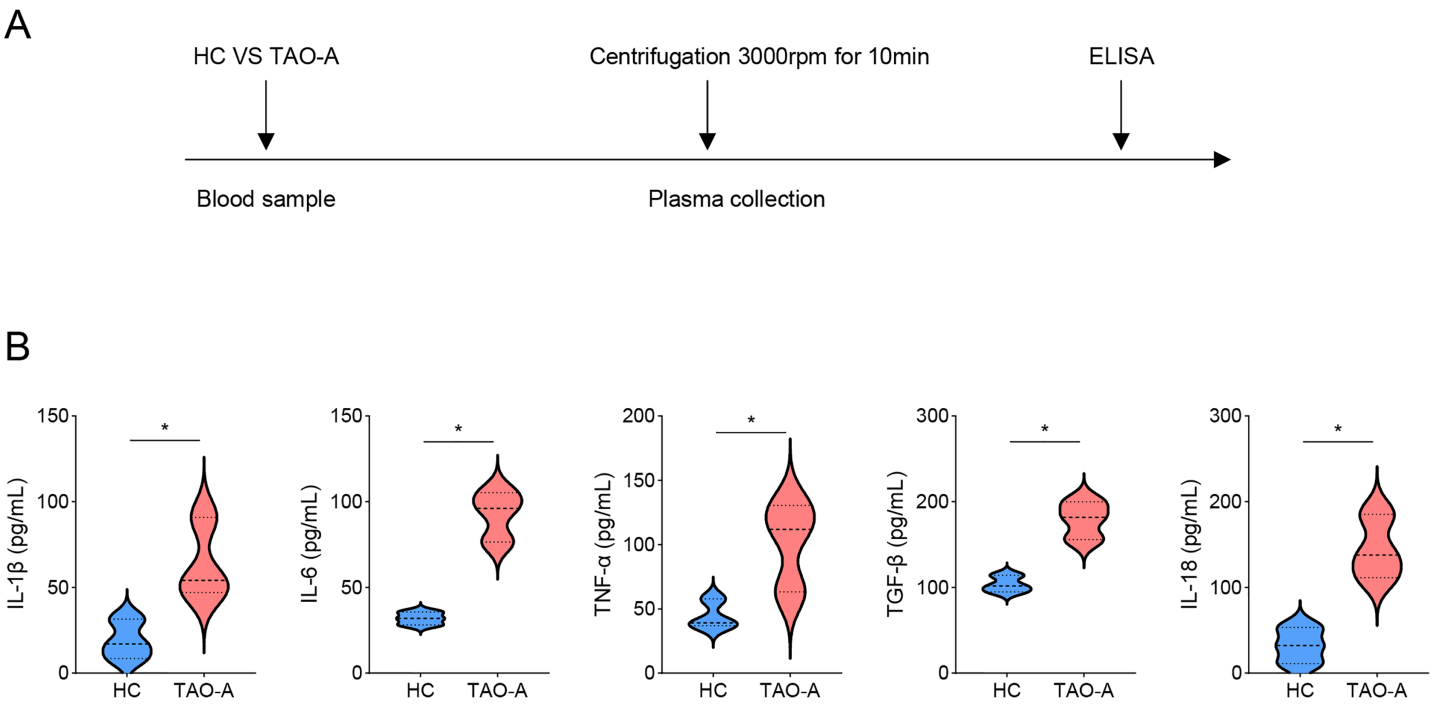


**Figure 1 Characterization on the plasma.** (A) The detailed procedures for plasma characterization. (B) The assay of ELISA was applied to calculate the levels of pro-inflammatory cytokines including IL-1β, IL-6, TNF-α, TGF-β and IL-18 in TAO-A patients and healthy control ($n$ = 5). Data are mean ± standard deviation from three independent experiments. *$p < 0.05$. Full-size DOI: 10.7717/peerj.18612/fig-1

### Statistical analysis

All the experiments were performed in independent triplicates and all the data were represented as mean ± standard deviation. Two-group differences were compared with unpaired student's $t$ tests. GraphPad Prism 6.0 software (GraphPad Software, Inc., La Jolla, CA, USA) was applied for statistical analysis. A $p$-value lower than 0.05 indicated a statistically significant difference.

## RESULTS

### Characterization on the plasma

Detailed procedures for plasma characterization were presented in Fig. 1A. ELISA was applied to calculate the levels of pro-inflammatory cytokines including IL-1β, IL-6, TNF-α, TGF-β and IL-18. Notably, the levels of these cytokines were relatively higher in the plasma from TAO-A patients as compared to those in HC (Fig. 1B, $p < 0.05$), indicating that the plasma from TAO-A patients had stronger pro-inflammatory properties.

### Effects of the plasma derived from TAO-A patients on the survival and migration of MAFs

The procedures for co-culturing MAFs with the plasmas of the two groups of patients were illustrated in Fig. 2A. Next, the effects of these plasmas on the survival and migration of

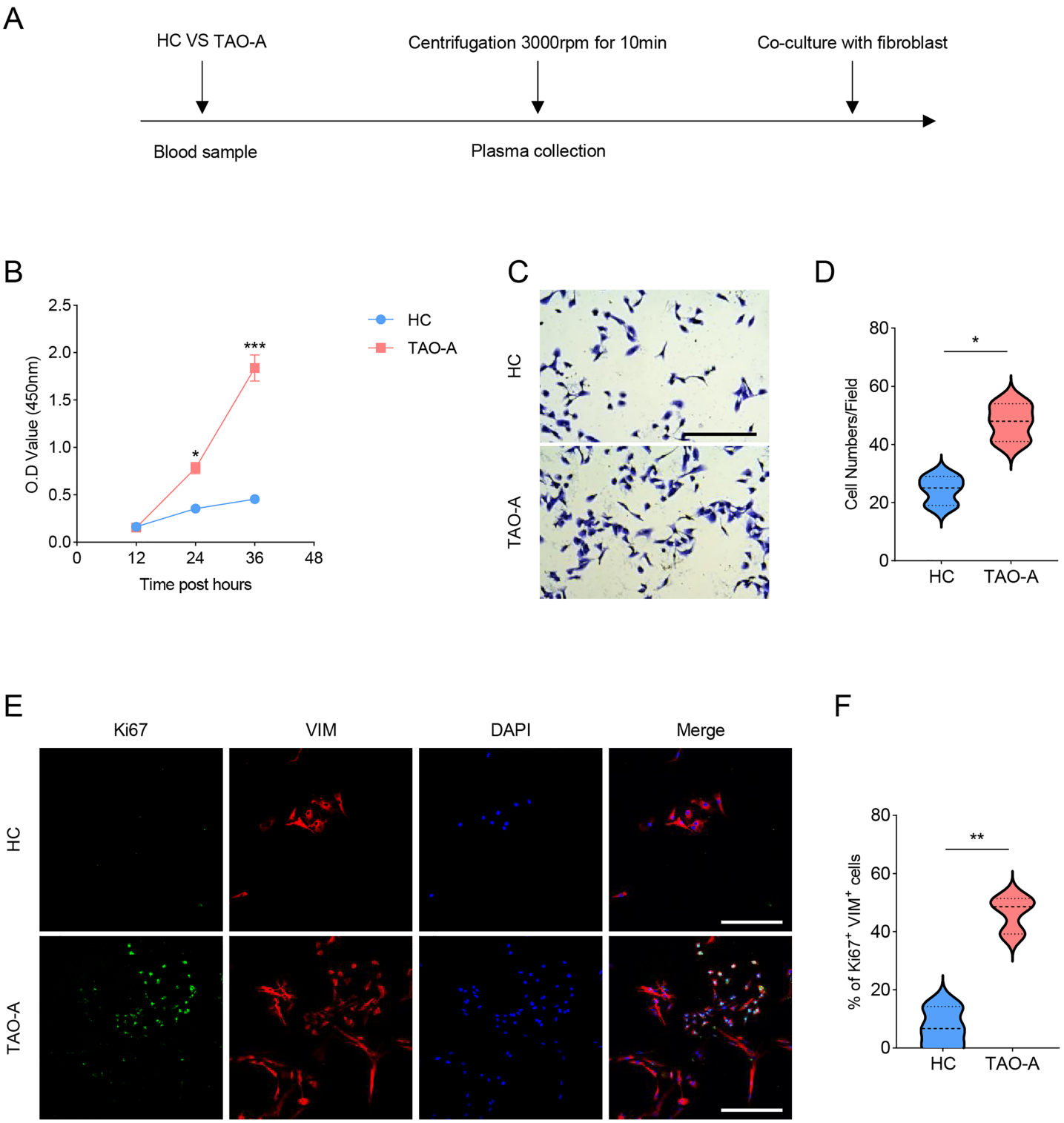


**Figure 2 Effects of TAO-A patients-derived plasma on the survival and migration of MAFs.** (A) The detailed procedures for plasma co-culture with MAFs. (B) Relative viability of MAFs under different co-culture schemes at 12, 24 and 36 h. (C and D) Number of migrated MAFs under different co-culture schemes at 48 h. (E and F) Number of $Ki67^{+}VIM^{+}$ MAFs under different co-culture schemes based on immunofluorescence assay. The scale is 50 μm. Data are mean ± standard deviation from three independent experiments. $^{*}p < 0.05$, $^{**}p < 0.01$, $^{***}p < 0.001$.

Full-size DOI: 10.7717/peerj.18612/fig-2

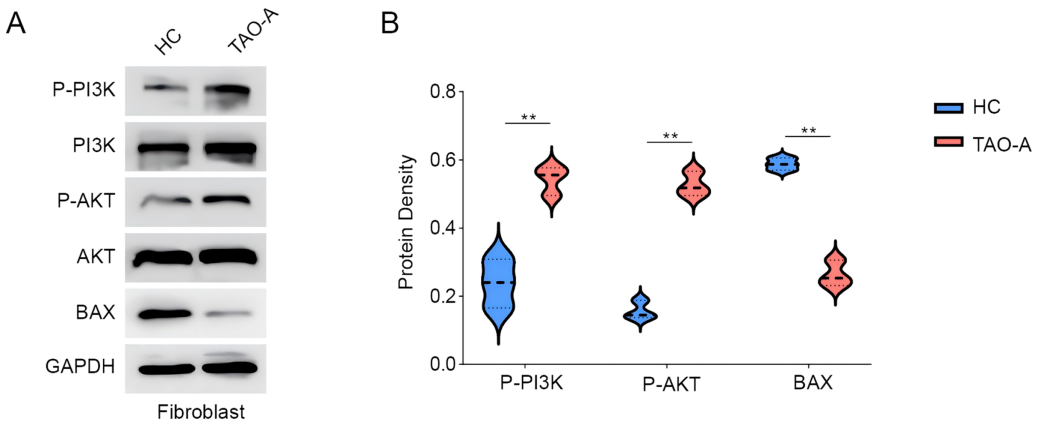


**Figure 3 Effects of TAO-A patients-derived plasma on proteins related to PI3K/AKT pathway and apoptosis in MAFs.** (A and B) Effects of TAO-A patients-derived plasma on proteins related to PI3K/AKT pathway and apoptosis in different groups of MAFs were explored based on the results of western blotting assay. Data are mean ± standard deviation from three independent experiments. $^{**}p < 0.01$.
Full-size DOI: 10.7717/peerj.18612/fig-3

MAFs were explored. The relevant results from CCK-8 and Transwell assays demonstrated that the plasma of TAO-A patients could evidently promote the viability and migration of MAFs (Figs. 2B–2D, $p < 0.05$). Ki67 is a cell proliferation marker commonly used to mark proliferative cells (*Li et al., 2015*). VIM is an intermediate fiber protein widely expressed in fibroblasts and other mesenchymal cells (*Ostrowska-Podhorodecka & McCulloch, 2021*). Here, $Ki67^{+}VIM^{+}$ MAFs were the MAFs that were proliferative (Ki67-positive) and had fibroblast properties (VIM-positive). These double-positive cells represented a highly active class of MAFs involved in the structural support of the TME and accelerated the expansion of the TME and tumor progression through cell proliferation. Further, the results from immunofluorescence assay confirmed that the co-culture of the plasma from TAO-A patients increased the number of $Ki67^{+}VIM^{+}$ MAFs (Figs. 2E and 2F, $p < 0.01$).

## Effects of the plasma from TAO-A patients on proteins related to PI3K/AKT pathway in MAFs and apoptosis

Subsequently, we analyzed the relevant pathway and molecular mechanisms underlying the effects of the plasma from TAO-A patients on MAFs. PI3K/AKT pathway is involved in the regulation of cell survival and migration (*Ma et al., 2021*). Here, we focused on PI3K/AKT pathway and the phosphorylation of relevant proteins PI3K and AKT were measured accordingly. It was found that the plasma of TAO-A patients visibly enhanced the phosphorylation of the two proteins in MAFs (Figs. 3A and 3B, $p < 0.01$). Bax, an apoptosis-related protein, was additionally used to determine the effects of the plasma from TAO-A patients on MAFs, and the results showed that Bax was reduced in MAFs following the culture with the plasma derived from TAO-A patients (Figs. 3A and 3B, $p < 0.01$). These results suggested that the plasma from TAO-A patients inhibited the apoptosis of MAFs through PI3K/AKT signaling pathway.

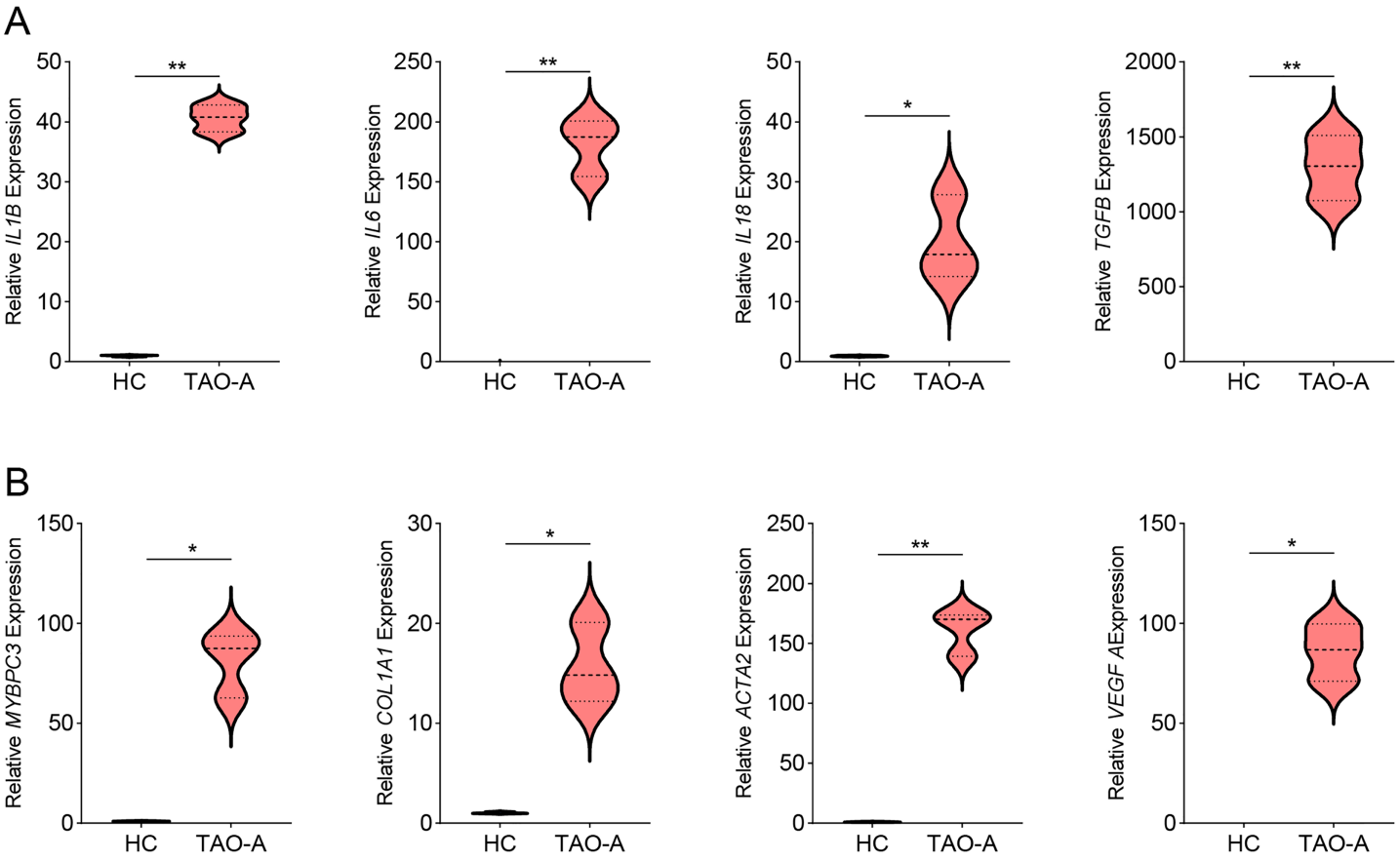


**Figure 4 Effects of TAO-A patients-derived plasma on inflammation-related and potential downstream genes in MAFs.** (A) Levels of pro-inflammatory cytokines in different groups of MAFs were calculated based on qPCR. (B) Levels of potential downstream genes in different groups of MAFs were calculated based on qPCR. Data are mean ± standard deviation from three independent experiments. *$p < 0.05$, **$p < 0.01$.

Full-size DOI: 10.7717/peerj.18612/fig-4

## Effects of the plasma derived from TAO-A patients on inflammation-related and potential downstream genes in MAFs

Then we measured the levels of genes related to inflammation in MAFs co-cultured with different types of plasma using qPCR, and observed that the co-culture with the plasma of TAO-A patients upregulated the expression of inflammatory cytokines including IL1B, IL6, IL18 and TGFB (Fig. 4A, $p < 0.05$) and that of the potential downstream genes MYBPC3, COL1A1, ACTA2 and VEGFA (Fig. 4B, $p < 0.05$). This indicated that the plasma from TAO-A patients enhanced the pro-inflammatory response of MAFs and their role in the TME.

## Effects of the plasma of TAO-A patients on M1 macrophage polarization

Additionally, the macrophage polarization status following the co-culture with different types of plasma was analyzed, and the co-culture procedures were shown in Fig. 5A. The macrophage polarization status was reflected by the mean fluorescence intensity (MFI) on CD86 (M1 polarization marker) and CD206 (M2 polarization indicator) using

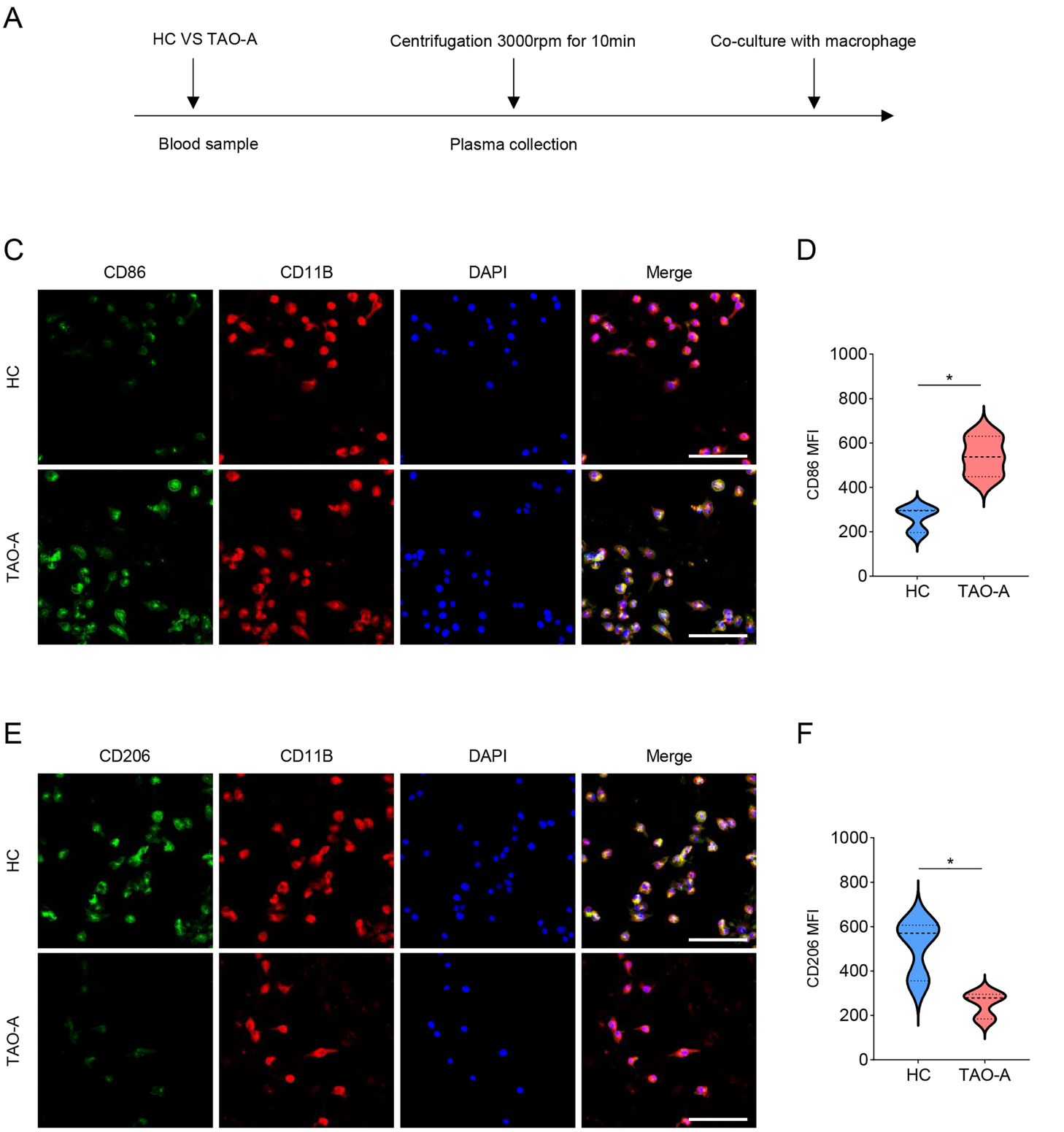


**Figure 5 Effects of TAO-A patients-derived plasma on M1 macrophage polarization.** (A) Co-culture schemes of induced macrophages with different groups of plasma. (B and C) CD86 MFI in macrophages co-cultured with different groups of plasma. (D and E) CD206 MFI in macrophages co-cultured with different groups of plasma. The scale is 50 μm. Data are mean ± standard deviation from three independent experiments. *$p < 0.05$.

Full-size DOI: 10.7717/peerj.18612/fig-5

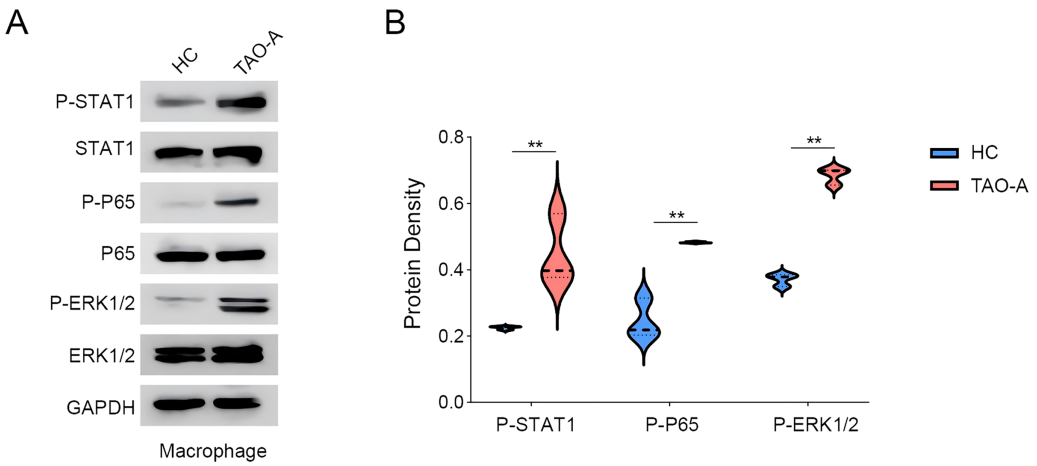


**Figure 6 Effects of TAO-A-patients-derived plasma on possible downstream pathways in macrophages.** (A and B) Relevant proteins to STAT, p65 and ERK pathways in macrophages following the co-culture were quantified based on western blotting assay. Data are mean ± standard deviation from three independent experiments. $^{**}p < 0.01$. Full-size DOI: 10.7717/peerj.18612/fig-6

immunofluorescence. According to the results of immunofluorescence assay, the plasma derived from TAO-A patients evidently enhanced the MFI of CD86 but reduced that of CD206 (Figs. 5B–5E, $p < 0.05$).

### Effects of the plasma derived from TAO-A patients on possible downstream pathways in macrophages

We explored the relevant proteins in macrophages following the co-culture, with a focus on STAT, p65 and ERK pathways. The activity of these signaling pathways was measured to assess whether the plasma from TAO-A patients enhanced the pro-carcinogenic properties of MAFs through the activation of these pathways to alter the TME and accelerate cancer progression. Based on Western blotting assay, it was found that the co-culture of the plasma from TAO-A patients enhanced the phosphorylation of STAT1, P65 and ERK1/2 (Figs. 6A and 6B, $p < 0.01$).

## DISCUSSION

TAO is a prevalent autoimmune inflammatory disorders in the orbit and a leading cause of orbital and strabismus symptoms to adults (*Kyriakos et al., 2022*; *Hennein & Robbins, 2022*). It has been noted that plasma exosomes from TAO-A patients could trigger inflammation in orbital fibroblasts (*Wei et al., 2024*). Based on previous findings, we speculated that the plasma from TAO-A patients could also initiate inflammation to promote the development of melanoma. In the current study, the effects of plasma from TAO-A patients on the survival of MAFs were analyzed, and it was observed that the plasma of TAO-A patients promoted the survival and migration of MAFs and enhanced M1 macrophage polarization, thereby accelerating melanoma progression *in vitro*.

Melanoma is one of the most aggressive and therapy-resistant cancers that has no adequate treatment available (*Shannan et al., 2016*; *Grossi et al., 2023*). The dynamic relationship between melanoma and fibroblast has the potential to improve the therapeutic

options for patients with the cancer (*Papaccio et al., 2021*). The current study used isolated MAFs to investigate their specific effects on melanoma progression. MAFs are involved in tumor-promoting inflammation and anti-tumor immunity (*Zhou et al., 2024*). Specifically, MAFs can reduce tumor cell susceptibility to natural killer cell-mediated killing *via* secreting matrix metalloproteinases (*Ziani et al., 2017*). Meanwhile, MAFs could also impair the function of $CD8^+$ T cells and modify the levels of immune checkpoint regulators by increasing arginase activity (*Érsek et al., 2021*). Additionally, mesenchymal-stromal cell-like MAFs increase IL-10 production by macrophages dependent on cyclooxygenase/indoleamine 2,3-dioxygenase (*Çakır et al., 2021*). As for the modulator of MAFs, it has been found that HSP90/IKK-rich small extracellular vesicles can activate those pro-angiogenic MAFs *via* the NF-κB/CXCL1 axis (*Tang et al., 2022*). In the current study, the co-culture of MAFs with the plasma from TAO-A patients evidently promoted the survival and migration of MAFs, as we observed that the cell viability and the numbers of migrated cells and $Ki67^+VIM^+$ MAFs were increased. Further exploration on the relevant pathways showed that the phosphorylation levels of PI3K and AKT in MAFs were elevated, indicating the potential involvement of PI3K/AKT pathway in the initiation and therapeutic resistance of melanoma (*Davies, 2012*).

Additionally, melanoma cells can interact with and are dependent on seemingly normal cells in their TME, thereby permitting the acquisition of their microenvironment (*Brandner & Haass, 2013*). In the context of skin cancers, there are some common characteristics of TME such as the presence of tumor-associated macrophages (*Georgescu et al., 2020*). Macrophages not only triggers the adaptive immune response and enhances the killing of tumor cells, but also promotes tumorigenesis and metastasis of melanoma when affected by the factors existing in the TME of melanoma (*Habib et al., 2024*). Further, mounting evidence indicated that macrophages can be classified into two distinctly different types (M1 and M2) (*Wang et al., 2017*). In the current study, elevated MFI of CD86 suggested M1 polarization in macrophages following the co-culture with the plasma from TAO-A patients, which was consistent with some existing studies describing the role of M1 macrophage in driving protumor inflammation of melanoma cells *via* TNFR-NF-κB signaling (*Kainulainen et al., 2022*). Further examination on the relevant pathways involved showed elevated levels of phosphorylation of STAT1, p65 and ERK1/2, which all participate in macrophage M1 polarization under diverse circumstances (*Kainulainen et al., 2022*; *Huangfu et al., 2020*; *Lu et al., 2023*).

## CONCLUSION

In conclusion, we demonstrated that the plasma from TAO-A patients profoundly influenced the survival and inflammation in MAFs. However, some limitations still existed in this study. For instance, this study only explored the effects of the plasma from TAO-A patients on the survival and inflammation of MAFs, but the specific molecules contributing to such effects were not investigated. Also, the study was conducted based on *in vitro* assays, therefore further *in vivo* experiments should be incorporated to validate the current findings.

## ABBREVIATIONS

| | |
|---|---|
| **TME** | tumor microenvironment |
| **CAFs** | cancer-associated fibroblasts |
| **MAFs** | Melanoma-associated fibroblasts |
| **TAO-A** | active thyroid-associated orbitopathy |
| **HC** | healthy control |
| **EDTA** | ethylenediaminetetraacetic acid |
| **PBS** | phosphate-buffered saline |
| **CCK-8** | cell counting kit-8 |
| **VIM** | Vimentin |
| **IL** | interleukin |
| **TNF** | tumor necrosis factor |
| **TGF** | transforming growth factor |
| **MFI** | mean fluorescence intensity |

## ADDITIONAL INFORMATION AND DECLARATIONS


### Funding

This project was supported by Guangxi Zhuang Autonomous Region Administration of Traditional Chinese Medicine (GXZYB20220329). The funders had no role in study design, data collection and analysis, decision to publish, or preparation of the manuscript.

### Grant Disclosures

The following grant information was disclosed by the authors:
Guangxi Zhuang Autonomous Region Administration of Traditional Chinese Medicine: GXZYB20220329.


### Competing Interests

The authors declare that they have no competing interests.

### Author Contributions

- Huifang Chen conceived and designed the experiments, performed the experiments, analyzed the data, prepared figures and/or tables, authored or reviewed drafts of the article, and approved the final draft.
- Shiyuan Chen conceived and designed the experiments, analyzed the data, prepared figures and/or tables, authored or reviewed drafts of the article, and approved the final draft.
- Zhenfeng Liu performed the experiments, analyzed the data, authored or reviewed drafts of the article, and approved the final draft.

### Human Ethics

The following information was supplied relating to ethical approvals (*i.e.*, approving body and any reference numbers):

The study was supported by Guangxi University of Science and Technology Medical Ethics Committee (No. YX20230301H015).

## Data Availability

The following information was supplied regarding data availability:

The raw data is available at GitHub, Zenodo, and figshare:

- https://github.com/1zf-gif/Raw-data.git

- 1zf-gif. (2024). 1zf-gif/Raw-data: Raw data (v.1.1.0). Zenodo. https://doi.org/10.5281/zenodo.13324703

- Chen, Huifang; Chen, Shiyuan; Liu, Zhenfeng (2024). Raw experimental data. figshare. Figure. https://doi.org/10.6084/m9.figshare.26793838.v1.

## Supplemental Information

Supplemental information for this article can be found online at http://dx.doi.org/10.7717/peerj.18612#supplemental-information.

# REFERENCES

**Ahmed B, Qadir MI, Ghafoor S. 2020.** Malignant melanoma: skin cancer-diagnosis, prevention, and treatment. *Critical Reviews in Eukaryotic Gene Expression* **30(4)**:291–297 DOI 10.1615/CritRevEukaryotGeneExpr.2020028454.

**Amuthalakshmi S, Sindhuja S, Nalini CN. 2022.** A review on PCR and POC-PCR—a boon in the diagnosis of COVID-19. *Current Pharmaceutical Analysis* **18(8)**:745–764 DOI 10.2174/1573412918666220509032754.

**Arneth B. 2019.** Tumor microenvironment. *Medicina (Kaunas, Lithuania)* **56(1)**:15 DOI 10.3390/medicina56010015.

**Bahn RS. 2010.** Graves' ophthalmopathy. *The New England Journal of Medicine* **362(8)**:726–738 DOI 10.1056/NEJMra0905750.

**Bellei B, Migliano E, Picardo M. 2020.** A framework of major tumor-promoting signal transduction pathways implicated in melanoma-fibroblast dialogue. *Cancers* **12(11)**:3400 DOI 10.3390/cancers12113400.

**Berchner-Pfannschmidt U, Moshkelgosha S, Diaz-Cano S, Edelmann B, Görtz GE, Horstmann M, Noble A, Hansen W, Eckstein A, Banga JP. 2016.** Comparative assessment of female mouse model of graves' orbitopathy under different environments, accompanied by proinflammatory cytokine and T-cell responses to thyrotropin hormone receptor antigen. *Endocrinology* **157(4)**:1673–1682 DOI 10.1210/en.2015-1829.

**Brandner JM, Haass NK. 2013.** Melanoma's connections to the tumour microenvironment. *Pathology* **45(5)**:443–452 DOI 10.1097/PAT.0b013e328363b3bd.

**Brenner M, Degitz K, Besch R, Berking C. 2005.** Differential expression of melanoma-associated growth factors in keratinocytes and fibroblasts by ultraviolet A and ultraviolet B radiation. *The British Journal of Dermatology* **153(4)**:733–739 DOI 10.1111/j.1365-2133.2005.06780.x.

**Çakır U, Hajdara A, Széky B, Mayer B, Kárpáti S, Mezey É, Silló P, Szakács G, Füredi A, Pós Z, Érsek B, Sárdy M, Németh K. 2021.** Mesenchymal-stromal cell-like melanoma-associated fibroblasts increase IL-10 production by macrophages in a cyclooxygenase/indoleamine 2,3-dioxygenase-dependent manner. *Cancers* **13(24)**:13–24 DOI 10.3390/cancers13246173.

**Davies MA. 2012.** The role of the PI3K-AKT pathway in melanoma. *Cancer Journal (Sudbury, Massachusetts)* **18(2)**:142–147 DOI 10.1097/PPO.0b013e31824d448c.

**Davis LE, Shalin SC, Tackett AJ. 2019.** Current state of melanoma diagnosis and treatment. *Cancer Biology & Therapy* **20(11)**:1366–1379 DOI 10.1080/15384047.2019.1640032.

**Eble JA, Niland S. 2019.** The extracellular matrix in tumor progression and metastasis. *Clinical & Experimental Metastasis* **36(3)**:171–198 DOI 10.1007/s10585-019-09966-1.

**Elhanani O, Ben-Uri R, Keren L. 2023.** Spatial profiling technologies illuminate the tumor microenvironment. *Cancer Cell* **41(3)**:404–420 DOI 10.1016/j.ccell.2023.01.010.

**Érsek B, Silló P, Cakir U, Molnár V, Bencsik A, Mayer B, Mezey E, Kárpáti S, Pós Z, Németh K. 2021.** Melanoma-associated fibroblasts impair CD8+ T cell function and modify expression of immune checkpoint regulators via increased arginase activity. *Cellular and Molecular Life Sciences: CMLS* **78(2)**:661–673 DOI 10.1007/s00018-020-03517-8.

**Georgescu SR, Tampa M, Mitran CI, Mitran MI, Caruntu C, Caruntu A, Lupu M, Matei C, Constantin C, Neagu M. 2020.** Tumour microenvironment in skin carcinogenesis. *Advances in Experimental Medicine and Biology* **1226**:123–142 DOI 10.1007/978-3-030-36214-0.

**Grossi LN, Braz WR, Silva NPd, Cazarim ELCC, Palmieri MGS, Tavares GD, Pittella F. 2023.** Ethosomes as delivery system for treatment of melanoma: a mini-review. *Oncologie* **25(5)**:455–459 DOI 10.1515/oncologie-2023-0177.

**Habib S, Osborn G, Willsmore Z, Chew MW, Jakubow S, Fitzpatrick A, Wu Y, Sinha K, Lloyd-Hughes H, Geh JLC, MacKenzie-Ross AD, Whittaker S, Sanz-Moreno V, Lacy KE, Karagiannis SN, Adams R. 2024.** Tumor associated macrophages as key contributors and targets in current and future therapies for melanoma. *Expert Review of Clinical Immunology* **20(8)**:1–17 DOI 10.1080/1744666X.2024.2326626.

**Hajdara A, Çakır U, Érsek B, Silló P, Széky B, Barna G, Faqi S, Gyöngy M, Kárpáti S, Németh K, Mayer B. 2023.** Targeting melanoma-associated fibroblasts (MAFs) with activated γδ (Vδ2) T cells: an in vitro cytotoxicity model. *International Journal of Molecular Sciences* **24(16)**:12893 DOI 10.3390/ijms241612893.

**Hennein L, Robbins SL. 2022.** Thyroid-associated orbitopathy: management and treatment. *Journal of Binocular Vision and Ocular Motility* **72**:32–46 DOI 10.1080/2576117X.2021.1991182.

**Huangfu N, Zheng W, Xu Z, Wang S, Wang Y, Cheng J, Li Z, Cheng K, Zhang S, Chen X, Zhu J. 2020.** RBM4 regulates M1 macrophages polarization through targeting STAT1-mediated glycolysis. *International Immunopharmacology* **83**:106432 DOI 10.1016/j.intimp.2020.106432.

**Junttila MR, de Sauvage FJ. 2013.** Influence of tumour micro-environment heterogeneity on therapeutic response. *Nature* **501(7467)**:346–354 DOI 10.1038/nature12626.

**Kainulainen K, Takabe P, Heikkinen S, Aaltonen N, de la Motte C, Rauhala L, Durst FC, Oikari S, Hukkanen T, Rahunen E, Ikonen E, Hartikainen JM, Ketola K, Pasonen-Seppänen S. 2022.** M1 macrophages induce protumor inflammation in melanoma cells through TNFR-NF-κB signaling. *The Journal of Investigative Dermatology* **142(11)**:3041–3051.e10 DOI 10.1016/j.jid.2022.04.024.

**Kyriakos G, Patsouras A, Voutyritsa E, Gravvanis C, Papadimitriou E, Farmaki P, Quiles-Sánchez LV, Georgakopoulou VE, Damaskos C, Ríos-Vergara A, Marín-Martínez L, Diamantis E. 2022.** The role of TPOAb in thyroid-associated orbitopathy: a systematic review. *Ocular Immunology and Inflammation* **30(7–8)**:1740–1746 DOI 10.1080/09273948.2021.1942498.

**Li LT, Jiang G, Chen Q, Zheng JN. 2015.** Ki67 is a promising molecular target in the diagnosis of cancer (review). *Molecular Medicine Reports* **11(3)**:1566–1572 DOI 10.3892/mmr.2014.2914.

**Lian W, Xiang P, Ye C, Xiong J. 2024.** Single-cell RNA sequencing analysis reveals the role of cancer-associated fibroblasts in skin melanoma. *Current Medicinal Chemistry* **31(42)**:7015–7029 DOI 10.2174/0109298673282799231211113347.

**Livak KJ, Schmittgen TD. 2001.** Analysis of relative gene expression data using real-time quantitative PCR and the 2(-Delta Delta C(T)) Method. *Methods (San Diego, California)* **25(4)**:402–408 DOI 10.1006/meth.2001.1262.

**Lu C, Cheng RJ, Zhang Q, Hu Y, Pu Y, Wen J, Zhong Y, Tang Z, Wu L, Wei S, Tsou PS, Fox DA, Li S, Luo Y, Liu Y. 2023.** Herbal compound cepharanthine attenuates inflammatory arthritis by blocking macrophage M1 polarization. *International Immunopharmacology* **125(Pt B)**:111175 DOI 10.1016/j.intimp.2023.111175.

**Ma L, Zhang R, Li D, Qiao T, Guo X. 2021.** Fluoride regulates chondrocyte proliferation and autophagy via PI3K/AKT/mTOR signaling pathway. *Chemico-Biological Interactions* **349**:109659 DOI 10.1016/j.cbi.2021.109659.

**Marzagalli M, Ebelt ND, Manuel ER. 2019.** Unraveling the crosstalk between melanoma and immune cells in the tumor microenvironment. *Seminars in Cancer Biology* **59(2)**:236–250 DOI 10.1016/j.semcancer.2019.08.002.

**Meng L, Zheng Y, Liu H, Fan D. 2024.** The tumor microenvironment: a key player in multidrug resistance in cancer. *Oncologie* **26**:41–58 DOI 10.1515/oncologie-2023-0459.

**Ostrowska-Podhorodecka Z, McCulloch CA. 2021.** Vimentin regulates the assembly and function of matrix adhesions. *Wound Repair and Regeneration: Official Publication of the Wound Healing Society [and] the European Tissue Repair Society* **29(4)**:602–612 DOI 10.1111/wrr.12920.

**Papaccio F, Kovacs D, Bellei B, Caputo S, Migliano E, Cota C, Picardo M. 2021.** Profiling cancer-associated fibroblasts in melanoma. *International Journal of Molecular Sciences* **22(14)**:7255 DOI 10.3390/ijms22147255.

**Park J, Luo Y, Park JW, Kim SH, Hong YJ, Lim Y, Seo YJ, Bae J, Seo SB. 2023.** Downregulation of DNA methylation enhances differentiation of THP-1 cells and induces M1 polarization of differentiated macrophages. *Scientific Reports* **13**:13132 DOI 10.1038/s41598-023-40362-8.

**Pitt JM, Marabelle A, Eggermont A, Soria JC, Kroemer G, Zitvogel L. 2016.** Targeting the tumor microenvironment: removing obstruction to anticancer immune responses and immunotherapy. *Annals of Oncology: Official Journal of the European Society for Medical Oncology* **27(8)**:1482–1492 DOI 10.1093/annonc/mdw168.

**Romano V, Belviso I, Venuta A, Ruocco MR, Masone S, Aliotta F, Fiume G, Montagnani S, Avagliano A, Arcucci A. 2021.** Influence of tumor microenvironment and fibroblast population plasticity on melanoma growth, therapy resistance and immunoescape. *International Journal of Molecular Sciences* **22(10)**:5283 DOI 10.3390/ijms22105283.

**Sala R, Jefferies WA, Walker B, Yang J, Tiong J, Law SK, Carlevaro MF, Di Marco E, Vacca A, Cancedda R, Cancedda FD, Ribatti D. 2002.** The human melanoma associated protein melanotransferrin promotes endothelial cell migration and angiogenesis in vivo. *European Journal of Cell Biology* **81(11)**:599–607 DOI 10.1078/0171-9335-00280.

**Schadendorf D, van Akkooi ACJ, Berking C, Griewank KG, Gutzmer R, Hauschild A, Stang A, Roesch A, Ugurel S. 2018.** Melanoma. *Lancet (London, England)* **392(10151)**:971–984 DOI 10.1016/S0140-6736(18)31559-9.

**Shannan B, Perego M, Somasundaram R, Herlyn M. 2016.** Heterogeneity in melanoma. *Cancer Treatment and Research* **167**:1–15 DOI 10.1007/978-3-319-22539-5.

**Shi A, Yan M, Pang B, Pang L, Wang Y, Lan Y, Zhang X, Xu J, Ping Y, Hu J. 2023.** Dissecting cellular states of infiltrating microenvironment cells in melanoma by integrating single-cell and bulk transcriptome analysis. *BMC Immunology* **24(1)**:52 DOI 10.1186/s12865-023-00587-8.

**Tagliaferri L, Lancellotta V, Fionda B, Mangoni M, Casà C, Di Stefani A, Pagliara MM, D'Aviero A, Schinzari G, Chiesa S, Mazzarella C, Manfrida S, Colloca GF, Marazzi F, Morganti AG, Blasi MA, Peris K, Tortora G, Valentini V. 2022.** Immunotherapy and radiotherapy in melanoma: a multidisciplinary comprehensive review. *Human Vaccines & Immunotherapeutics* **18(3)**:1903827 DOI 10.1080/21645515.2021.1903827.

**Tang H, Zhou X, Zhao X, Luo X, Luo T, Chen Y, Liang W, Jiang E, Liu K, Shao Z, Shang Z. 2022.** HSP90/IKK-rich small extracellular vesicles activate pro-angiogenic melanoma-associated fibroblasts via the NF-κB/CXCL1 axis. *Cancer Science* **113(4)**:1168–1181 DOI 10.1111/cas.15271.

**Wang Y, Liu Y, Cai J, Zong T, Zhang Z, Xie T, Mu T, Wu M, Yang Q, Wang Y, Wang X, Yao Y. 2023.** Differentially expressed genes in orbital adipose/connective tissue of thyroid-associated orbitopathy. *PeerJ* **11(8)**:e16569 DOI 10.7717/peerj.16569.

**Wang Y, Sharma A, Padnick-Silver L, Francis-Sedlak M, Holt RJ, Foley C, Massry G, Douglas RS. 2021.** Physician-perceived impact of thyroid eye disease on patient quality of life in the United States. *Ophthalmology and Therapy* **10(1)**:75–87 DOI 10.1007/s40123-020-00318-x.

**Wang H, Yang L, Wang D, Zhang Q, Zhang L. 2017.** Pro-tumor activities of macrophages in the progression of melanoma. *Human Vaccines & Immunotherapeutics* **13(7)**:1556–1562 DOI 10.1080/21645515.2017.1312043.

**Wei L, Huang Q, Tu Y, Song S, Zhang X, Yu B, Liu Y, Li Z, Huang Q, Chen L, Liu B, Xu S, Li T, Liu X, Hu X, Liu W, Chi ZL, Wu W. 2024.** Plasma exosomes from patients with active thyroid-associated orbitopathy induce inflammation and fibrosis in orbital fibroblasts. *Journal of Translational Medicine* **22(1)**:546 DOI 10.1186/s12967-024-05263-y.

**Xiao Y, Yu D. 2021.** Tumor microenvironment as a therapeutic target in cancer. *Pharmacology & Therapeutics* **221**:107753 DOI 10.1016/j.pharmthera.2020.107753.

**Zhang J, He J, Chen W, Chen G, Wang L, Liu Y, Wang Z, Yang M, Huang G, Yang Y, Ma W, Li Y. 2024.** Single-cell RNA-binding protein pattern-mediated molecular subtypes depict the hallmarks of the tumor microenvironment in bladder urothelial carcinoma. *Oncologie* **26(4)**:657–669 DOI 10.1515/oncologie-2024-0071.

**Zhou Q, Jin X, Zhao Y, Wang Y, Tao M, Cao Y, Yin X. 2024.** Melanoma-associated fibroblasts in tumor-promotion flammation and antitumor immunity: novel mechanisms and potential immunotherapeutic strategies. *Human Molecular Genetics* **33(13)**:1186–1193 DOI 10.1093/hmg/ddae056.

**Ziani L, Safta-Saadoun TB, Gourbeix J, Cavalcanti A, Robert C, Favre G, Chouaib S, Thiery J. 2017.** Melanoma-associated fibroblasts decrease tumor cell susceptibility to NK cell-mediated killing through matrix-metalloproteinases secretion. *Oncotarget* **8(12)**:19780–19794 DOI 10.18632/oncotarget.15540.